Boletín de la Sociedad Española de Cerámica y Vidrio
Vol 53, 4, 179-193, Julio-Agosto 2014 ISSN 0366-3175. eISSN 2173-0431.
http://dx.doi.org/10.3989/cyv.222014

BOLETIN DE LA SOCIEDAD ESPAÑOLA DE
Cerámica y Vidrio
A R T I C U L O

Synthesis of $Ba_{0.75}Sr_{0.25}Al_2Si_2O_8$ - ZrO_2 Ceramic Composites by Solid State Reaction of Mechanically Activated Precursor Mixtures

M.V. RAMOS-RAMÍREZ, J. LÓPEZ-CUEVAS*, J.L. RODRÍGUEZ-GALICIA AND J.C. RENDÓN-ANGELES

CINVESTAV-IPN, Unidad Saltillo, Calle Industria Metalúrgica, Número 1062,
Parque Industrial Saltillo - Ramos Arizpe, Ramos Arizpe, Coahuila, México, CP 25900
*Corresponding author. Tel. +52 844 4389600; fax: +52 844 4389610. E-mail address: jorge.lopez@cinvestav.edu.mx (J. López-Cuevas)

Precursor mixtures composed of fly ash, $BaCO_3$, $SrCO_3$, Al_2O_3 and ZrO_2, were subjected to attrition milling for 0-8 h and then uniaxially pressed and sintered at 900-1500 °C/5 h, for the *in situ* solid state synthesis of composites with nominal $Ba_{0.75}Sr_{0.25}Al_2Si_2O_8$ (SBAS)/ZrO_2 mass ratios of: 1) 90/10, 2) 70/30, and 3) 50/50. Mechanical activation, combined with the likely generation of a considerable amount of transient liquid during sintering of the composites, notably enhanced the reactivity of the precursor mixtures. ZrO_2 decreased the conversion from the hexagonal (Hexacelsian) into the monoclinic (Celsian) phases of SBAS in the composites, which became more pronounced when the content of ZrO_2 was increased in the materials. Nearly full conversions could be achieved at temperatures as low as 1100 °C, by mechanically activating the precursor mixtures for times that increased with increasing content of ZrO_2 in the materials. An increment in the time of mechanical activation of the precursor mixtures, as well as in their ZrO_2 content and in the sintering temperature, increased the mechanical properties of the synthesized materials. Thus, the best mechanical properties were obtained for composition 3 milled for 8 h and sintered at 1500 °C.

Keywords: Mechanical activation; Solid state reaction; Fly ash; Celsian; Mechanical properties.

Síntesis de compósitos cerámicos $Ba_{0.75}Sr_{0.25}Al_2Si_2O_8$ - ZrO_2 por reacción en el estado sólido de mezclas precursoras activadas mecánicamente

Mezclas precursoras de cenizas volantes, $BaCO_3$, $SrCO_3$, Al_2O_3 y ZrO_2, fueron activadas mecánicamente en un molino de atrición por 0-8 h y luego prensadas uniaxialmente y sinterizadas a 900-1500 °C/5 h, para la síntesis *in situ* por reacción en el estado sólido de compósitos con relaciones nominales $Ba_{0.75}Sr_{0.25}Al_2Si_2O_8$ (SBAS)/ZrO_2 en masa de: 1) 90/10, 2) 70/30, y 3) 50/50. La activación mecánica, combinada con la probable generación de una cantidad considerable de líquido transitorio, incrementó notablemente la reactividad de las mezclas precursoras. La ZrO_2 disminuyó la conversión de la fase hexagonal (Hexacelsiana) a la monoclínica (Celsiana) del SBAS, lo cual fue más pronunciado cuando el contenido de ZrO_2 se incrementó en los compósitos. Fue posible obtener conversiones casi completas a temperaturas tan bajas como 1100 °C, activando mecánicamente las mezclas precursoras por tiempos que se incrementaron con el incremento en el contenido de ZrO_2 en los materiales. El incremento en el tiempo de activación mecánica de las mezclas precursoras, así como en su contenido de ZrO_2 y en la temperatura de sinterización, incrementó las propiedades mecánicas de los materiales sintetizados. Así, las mejores propiedades mecánicas correspondieron a la composición 3 molida por 8 h y sinterizada a 1500 °C.

Palabras clave: Activación Mecánica; Reacción en el estado sólido; Cenizas Volantes; Celsiana; Propiedades mecánicas.

Cómo citar este artículo: Ramos-Ramírez, M. V.; López-Cuevas, J.; Rodríguez-Galicia, J. L.; Rendón-Angeles, J. C. (2014): Synthesis of $Ba_{0.75}Sr_{0.25}Al^2Si_2O_8$ - ZrO_2 Ceramic Composites by Solid State Reaction of Mechanically Activated Precursor Mixtures, *Bol. Soc. Esp. Ceram. Vidr.*, 53 (4): 179-193. http://dx.doi.org/10.3989/cyv.222014

1. INTRODUCTION

$BaAl_2Si_2O_8$ (BAS) and its solid solutions with SrO (SBAS, $Ba_{1-x}Sr_xAl_2Si_2O_8$) are attractive as matrixes for ceramic composites for structural applications at high temperatures, especially in their monoclinic polymorphic form known either as Celsian or as Monocelsian. However, in both materials an undesirable hexagonal polymorphic form known as Hexacelsian tends to appear prior to Celsian, remaining frequently in a metastable state at low temperatures. Hexacelsian has a coefficient of thermal expansion (CTE) higher than that of Celsian, and it might undergo a conversion into an orthorhombic phase at ~300 °C, causing a differential volume change of ~3-4 % that leads to microcracking of the material, with a deleterious effect on its final mechanical properties (1,2). The conversion of Hexacelsian into Celsian tends to be difficult and sluggish, especially in the case of BAS, since this conversion is easier in SBAS due to its content of SrO. The stabilization of Celsian can also be achieved by doping the material with mineralizing agents such as Li_2O, NaF, CaO, TiO_2, MgO, SrF_2, BeO and Cr_2O_3 (3,4). The BAS and SBAS-based composite materials are employed in structural applications such as environmental barrier coatings (EBCs) for Si-based (SiC, Si_3N_4) ceramic components in the hot section of advanced gas turbine engines (5).

Regarding the BAS-ZrO_2 and SBAS-ZrO_2 composites in which BAS and SBAS are present as Celsian, which are of particular interest in this work, we found that while some studies have been reported on the former composites (6-11), no information whatsoever has been published in relation with the latter materials. However, the results that have been reported for BAS-ZrO_2 composites could serve as a starting point for the study of SBAS-ZrO_2 compositions. It is known that BAS and ZrO_2 are chemically compatible, in such a way that they are able to coexist at equilibrium over a broad temperature range (6-10). It has been suggested (6) that for the BAS-ZrO_2 composites enhanced fracture toughness may result from the tetragonal (t-ZrO_2) to the monoclinic (m-ZrO_2) transformation of ZrO_2, in a manner analogous to other ZrO_2-toughened ceramics. It has also been reported (7) that Hexacelsian can accept ~10 mol. % of ZrO_2 in solid solution at 1050 °C, and that Celsian may also take a small amount of ZrO_2 in solid solution at 1200 °C (6). It has been observed that ZrO_2 influences the crystalline structure of BAS, since it tends to favor the formation of Hexacelsian. An analysis of the results reported by Khater and Idris (4), Debsikdar and Sowemimo (7), Sandhage et al. (6,11), and Yu-Feng et al. (12), suggested that the formation of Hexacelsian is promoted by ZrO_2 contained in the materials in a broad concentration range, at relatively low sintering or crystallization temperatures, especially in the case of non-stoichiometric BAS compositions, and especially in the absence in the materials of Celsian seeding, fluxes and/or mineralizing agents. The easier formation of Celsian in the presence of fluxes could be related with the formation of transient liquids, with a likely simultaneous enhancement of diffusivity in the materials. Sandhage and Fraser (6) mentioned that a faster conversion from the hexagonal into the monoclinic forms of BAS was associated with the presence of an amorphous silicate in the sintered materials, which should have been liquid at the treatment temperatures. Such liquid could enhance the mentioned conversion via a dissolution/reprecipitation mechanism. Khater and Idris (4), who studied the addition of small amounts of ZrO_2 to a Li-Ba aluminosilicate glass, mentioned that ZrO_2 increased the viscosity of the glass, reducing the mobility of its structural groups. Thus, the transformation between the complex aluminosilicate structures (i.e., Hexacelsian to Celsian) was delayed by the addition of ZrO_2. Lastly, the mechanical activation of the precursor mixtures prior to the solid-state synthesis of BAS is also known to promote the formation of Hexacelsian (13). It was hypothesized that the very fine particles with fresh surfaces created by the milling process provide the necessary conditions for the surface nucleation of Hexacelsian.

The stabilization of Celsian in SBAS-matrix composites under the combined influence of mechanical activation together with the presence of ZrO_2 and mineralizing agents in the materials has not been previously reported. In this work, we studied the *in situ* synthesis of $Ba_{0.75}Sr_{0.25}Al_2Si_2O_8$ (SBAS) - ZrO_2 composites by solid state reaction employing fly ash (FA, silicoaluminous byproduct of a Mexican coal-burning power plant), $BaCO_3$, $SrCO_3$, Al_2O_3 and ZrO_2 as raw materials, with the precursor mixtures subjected to prior mechanical activation. The main objective of this work was to study the dependence of the phase composition, and physical and mechanical properties of the synthesized composite materials, on the nominal SBAS/ZrO_2 mass ratio, as well as on the conditions employed for the mechanical activation given to the initial mixtures of raw materials and temperature used for their posterior reactive sintering.

2. EXPERIMENTAL PROCEDURE

2.1 Preparation of precursor mixtures

$Ba_{0.75}Sr_{0.25}Al_2Si_2O_8$ (SBAS)-ZrO_2 composites with nominal SBAS/ZrO_2 mass ratios of: 1) 90/10, 2) 70/30, and 3) 50/50, were *in situ* synthesized by solid state reaction. These materials are hereinafter referred to as compositions 1, 2 and 3, respectively. The raw materials employed were: Coal fly ash (FA); Al_2O_3 (with purity of 99.99 wt. % and particle size <1 μm, SASOL HPA-0.5, USA); 3 mol. % Y_2O_3-stabilized ZrO_2 (with purity of 99.99 wt. % and particle size <0.5 μm, Inframat Advaced Materials, USA); $BaCO_3$ (with purity of 99.43 wt. % and particle size of ~3 μm, Alkem, México), and $SrCO_3$ (with purity of 97.83 wt. % and particle size of ~4 μm, Solvay, México). Except for the employed FA, all the other materials were used as received. The phase composition of all initial and synthesized materials was analyzed by means of X-Ray Diffraction (XRD) using a Philips X'Pert 3040 XRD apparatus, with CuK_α radiation (λ = 1.54 Å), accelerating voltage of 40 kV, current of 30 mA, and a step size of 0.03° (2θ/s). This analysis showed that the 3 mol. % Y_2O_3-stabilized ZrO_2 predominantly t-ZrO_2. The particle size of all materials was determined by laser diffraction using a Coulter LS-100 apparatus.

After milling for 1 h in a ball mill, the original content of iron oxides of the FA was reduced in ~45 wt. % by means of a manual wet magnetic separation process using a neodymium magnet with an intensity of 12,300 Gauss. This was carried out in order to reduce the level of impurities contained in the FA. The iron oxides present in the FA come from the coal used to generate it, and these oxides are better eliminated if they are liberated first from the glassy matrix surrounding them in the FA, which could be achieved by milling this material prior to carry out the magnetic separation process. The chemical composition of the FA was determined before and after the magnetic separation process by means of semiquantitative short wavelength dispersive X-Ray Fluorescence (XRF) spectroscopy using a S4 Pioneer Bruker apparatus. The chemical composition of the conditioned FA was (wt. %): 64.48 % SiO_2, 27.28 % Al_2O_3, 2.33 % Fe_2O_3, 2.44 % CaO, 0.64 % MgO, 0.62 % TiO_2, 0.28 % K_2O, 0.18 % Na_2O, and 0.19 % of other oxides (ZrO_2, MnO_2, SrO, PbO and P_2O_5). Thermogravimetry (TGA) revealed that it also contained 1.73 % of free C. All TGA/DTA thermal analyses performed throughout this work were carried out up to 1400 °C, employing a Perkin Elmer Pyris Diamond simultaneous TGA/DTA apparatus, platinum crucibles and a heating rate of 10 °C/min, under still ambient air. The XRD analysis indicated that both the as-received and the conditioned FA were mostly composed of α-quartz and mullite ($Al_6Si_2O_{13}$). Dissolution of the conditioned FA with HF acid (14) allowed us to estimate that it also contained ~70 wt. % of a silicoaluminous glassy phase. Since both the as-received and the conditioned FA had a content of SiO_2 + Al_2O_3 + Fe_2O_3 above 70 wt. %, it was determined that the used FA belonged to the F type, according to the ASTM C618 standard (15). The mean particle size of the conditioned FA was ~30 μm.

The proportions of conditioned FA (hereinafter denominated simply as "FA"), Al_2O_3, $BaCO_3$, $SrCO_3$ and ZrO_2 required for the preparation of the stoichiometric mixtures

employed for the synthesis of the studied ceramic composites, hereinafter denominated simply as "precursor mixtures", are shown in Table I.

TABLE I. COMPOSITION (WT. %) OF THE PRECURSOR MIXTURES EMPLOYED FOR THE SYNTHESIS OF THE STUDIED CERAMIC COMPOSITES.

Composition	FA	Al_2O_3	$BaCO_3$	$SrCO_3$	ZrO_2
1	39.17	11.70	32.05	8.09	8.99
2	31.04	9.37	25.53	6.49	27.57
3	23.34	6.43	18.51	4.65	47.07

2.2 Mechanical activation of precursor mixtures

The precursor mixtures were milled for 0, 4 or 8 h in a Teflon-lined closed chamber laboratory attrition mill operated at 1700 rpm, employing 8 mol. % MgO partially-stabilized ZrO_2 balls as milling media, with a diameter of 1 mm, using a balls to load mass ratio of 5:1 as well as ethylic alcohol as dispersion medium. The mean particle size of the precursor mixtures decreased from the range of ~17-23 μm to the range of ~5-9 μm after 8 h of milling. At a given milling time, the mean particle size of the precursor mixture decreased with increasing content of ZrO_2 in it, which was due to the fact that this was the constituent with the smallest initial mean particle size.

All green precursor mixtures, with or without mechanical activation, were analyzed by simultaneous Thermogravimetry/Differential Thermal Analysis (TGA/DTA). The derivative thermogravimetric (DTG) curves were also determined for all compositions and milling times employed. For this, a relative weight loss (α) was defined as:

$$\alpha = \frac{W_0 - W_t}{W_0 - W_f} \quad (1)$$

where W_0 = initial weight (mg), W_t = weight at time t (mg), and W_f = final weight (mg) of the sample.

2.3 Solid state reaction

Prior to reactive sintering, a portion of each one of the precursor mixtures, with or without mechanical activation, was uniaxially pressed into 1.5g-cylinders with a diameter of 1.2 cm and a height of 0.5 cm, applying a load of 4 Ton, using for this a Carver Inc. 4350 press. Then, the cylinders were sintered for 5 h at temperatures from 900 ºC to 1500 °C, in steps of 200 °C, using a Thermolyne 46120-CM-33 high temperature electric furnace, employing heating and cooling rates of 2 and 5 °C/min, respectively. The rest of the powders of all compositions were uniaxially pressed into prismatic bars with a length of 7 cm, a width of 3 cm, and a height of 5 cm, applying a load of 7 Ton. Then, the prismatic bars were sintered for 8 h, due to their much larger size with respect to the cylindrical specimens, using the same temperatures and equipment mentioned before. In all cases, the furnace was turned off after the sintering treatment, allowing the samples to cool down to room temperature in a natural way inside the furnace.

2.4. Phase composition of the sintered materials

All sintered materials were analyzed by means of XRD and Scanning Electron Microscopy (SEM/EDS). For microstructural analysis, the sintered cylinders were cross-sectioned by using a diamond saw. Then, one half of each sample was mounted in cold-cure epoxy resin and the cut surface was ground using SiC papers with successive grit sizes from 80 grit to 2400 grit. The ground surface was then polished to a mirror finish using diamond particles with successive sizes of 3, 1 and ¼ μm, which was followed by graphite-coating of the polished surface using a JEOL JEE-400 vacuum evaporator. All observations on the SEM were carried out using a JEOL-6300 SEM, with an accelerating voltage of 15 KV and a working distance of 8 mm. For the XRD analyses, the remnant halves of the sintered cylinders were crushed using a synthetic sapphire mortar and pestle, until a particle size of 25-75 μm was achieved. This operation was carried out carefully trying not to appreciably change the m-ZrO_2/t-ZrO_2 ratio in the sintered samples.

XRD was also used in order to quantify all the phases detected in the sintered samples, with the aid of the XPowder 2004.04 software, which uses non-linear least squares methods and weighting achieved by means of the normalized RIR method described by Chung (16). The Hexacelsian to Celsian conversion fraction (f, %) was calculated using the weight percentages determined by XRD for both phases, together with the following expression:

$$f = \left(\frac{\%Celsian}{\%Celsian + \%Hexacelsian} \right) x100 \quad (2)$$

2.5. Evaluation of physical properties of the sintered materials

The relative density (ρ_r) of the sintered cylinders and prismatic bars was determined with or without mechanical activation of the initial precursor mixtures. No significant differences were observed between the density values obtained for both types of samples with same composition and same milling and sintering conditions. The value of ρ_r was determined by using equation 3:

$$\rho_r = \frac{\rho_A}{\rho_T} \quad (3)$$

where ρ_A = apparent density of the material (g/cm³) determined by the Archimedes' principle in distilled water at room temperature (~25 °C), and ρ_T = theoretical density of the material (g/cm³) calculated for the studied nominal composite compositions by using the Rule of Mixtures and a density of 3.314 g/cm³ for monoclinic $Ba_{0.75}Sr_{0.25}Al_2Si_2O_8$ taken from the JCPDS card no. 38-1451, as well as a density of 6.10 g/cm³ reported for 3 mol. % Y_2O_3-stabilized ZrO_2 by the supplier of this material. Since the JCPDS card corresponding to the hexagonal $Ba_{0.75}Sr_{0.25}Al_2Si_2O_8$ phase was not found, a density value of 3.257 g/cm³ was estimated for it by linear fitting of the density values reported in the JCPDS cards no. 88-1048, 26-0182, 26-0183, 26-0184 and 35-0073, for hexagonal $Ba_{1-x}Sr_xAl_2Si_2O_8$ solid solutions with x = 0, 0.1, 0.5, 0.9 and 1, respectively. Although the density estimated for the hexagonal $Ba_{0.75}Sr_{0.25}Al_2Si_2O_8$ phase is only ~1.72 % smaller than that

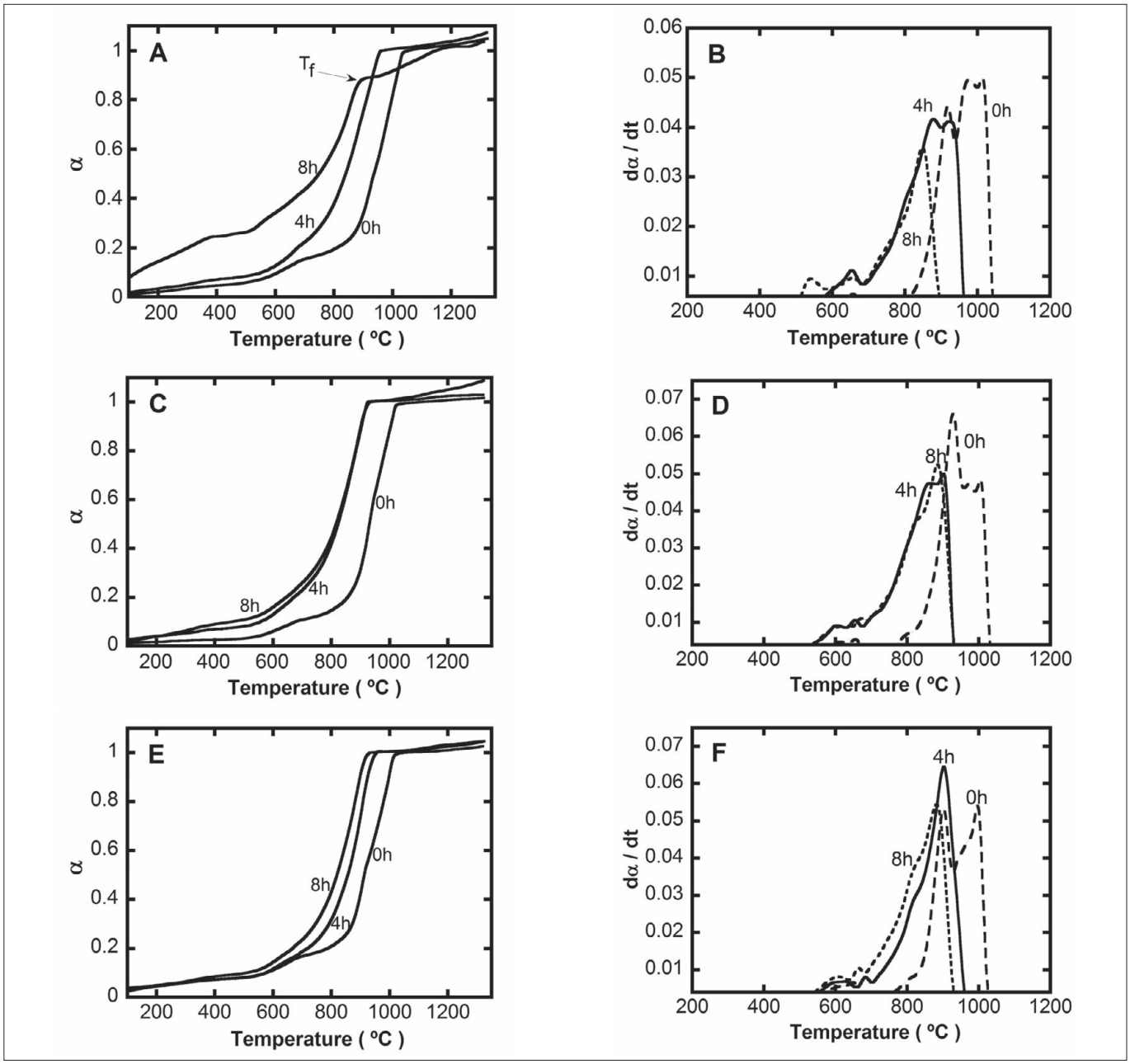

Figure 1. TGA (a,c,e) and DTG (b,d,f) curves obtained for the precursor mixtures of compositions 1 (a,b), 2 (c,d), and 3 (e,f) mechanically activated for the three milling times employed. T_f = Temperature at which the main weight loss stage finishes in the materials.

of the monoclinic phase, only the latter one was used for the calculation of the theoretical density of the composite materials, since we intended to obtain full Hexacelsian to Celsian conversions in them.

The CTE of sample bars with dimensions of 40x5x5 mm, which were cut from the sintered prismatic bars by using a diamond saw, was determined from room temperature up to 1200 °C by using a Netzch DIL 402 PC dilatometer, employing an alumina rod as standard.

2.6. Evaluation of mechanical properties of the sintered materials

The mechanical properties (Young's modulus, modulus of rupture (MOR), fracture toughness (K_{IC}), and Vickers microhardness (HV)) of the sintered materials were evaluated using the equipment and methods described in detail elsewhere (17). Briefly, the Young's modulus was evaluated by using a pulso-echo ultrasonic inspection technique (18) and alternatively by four-point flexural strength testing (19). The MOR was evaluated according to the ASTM C1161-02 standard (20). K_{IC} was evaluated according to the ASTM STP601 standard (21,22). Lastly, the Vickers microhardness was determined according to the ASTM E384-99 standard (23).

3. RESULTS AND DISCUSSION

3.1. Thermal analysis of the precursor mixtures

The TGA curves showed, Figure 1(a,c,e), that all samples started losing weight since the very beginning of the heating

Bol. Soc. Esp. Ceram. Vidr. Vol 53. 4, 179-193, Julio-Agosto 2014. ISSN 0366-3175. eISSN 2173-0431. http://dx.doi.org/10.3989/cyv.222014

stage, which was probably due to the release of small amounts of water adsorbed on the surface of the particles. It was also observed that the rate of weight loss increased with increasing mechanical activation; i.e., at a given temperature the weight loss increased with increasing milling time. In all cases, the main weight loss stage finished when a certain temperature (T_f) was reached, whose magnitude decreased with increasing milling time. This implies that mechanical activation caused a shifting in the weight loss stage of the materials towards lower temperatures, which was probably due to an acceleration of the solid-state reaction rate. However, in all cases the experimental total weight loss was very close to the theoretical value, see Table II. After 8 h of milling, in the case of composition 1 T_f decreased from ~1033 ºC to ~887 ºC (ΔT_f = 146 °C), Figure 1(a), while for compositions 2 and 3 T_f decreased from ~1021 ºC to ~928 ºC (ΔT_f = 93 °C), and from ~1019 ºC to ~922 ºC (ΔT_f = 97 °C), respectively, Figures 1(c,e). Since composition 1 had the largest ΔT_f value, this suggests that this composition achieved the highest degree of mechanical activation, which was probably related to the fact that it had the highest content of $BaCO_3$ and $SrCO_3$ in it. This could be attributed to the high degree of disorder introduced in the crystalline structure of both carbonates by the high-energy milling, as well as to the high degree of homogeneity and small particle size achieved by the materials as a result of mechanical activation (24,25). This not only decreased the temperature and the activation energy required for the thermal decomposition of both carbonates, but also increased their reactivity in the solid state towards other materials mixed with them (26-30).

TABLE II. THEORETICAL AND EXPERIMENTAL WEIGHT LOSSES OBTAINED FOR THE STUDIED PRECURSOR MIXTURES.

Composition	Total weight loss (%)	
	Theoretical*	Experimental**
1	10.16	11.03
2	8.10	8.83
3	5.87	6.33

*Includes CO_2 released by both $BaCO_3$ and $SrCO_3$, as well as the loss on ignition of the employed FA.
**Mean values of the total weight losses obtained for the three milling times employed.

Figure 1(b,d,f) shows that as the milling time increased, the DTG curves of all the studied materials became less complex, involving a smaller number of peaks, which was probably associated with the occurrence of a smaller number of reaction steps. At the same time, the DTG curves were shifted towards lower temperatures. This indicates that the reactivity of the precursor mixtures and the kinetics of the reactions associated with the observed weight losses increased with increasing milling time, in such a way that those reactions took place at lower temperatures in the milled materials, in comparison with the non-mechanically activated mixtures. The peaks located at ~500-700 °C were attributed to the thermal decomposition of hydrated compounds, such as $Sr(OH)_2$ or $Sr(HCO_3)_2$, likely formed shortly after the freshly milled materials made contact with the air's moisture (27,28,31). Further weight losses in this temperature range could be caused by combustion of the free carbon contained in the employed FA (32). The peaks located at ~700-900 °C were attributed to solid-state reactions for the formation of transient barium silicates and aluminate, Hexacelsian and Celsian. On the other hand, the peaks located at ~900-1500 °C were attributed to the thermal decomposition of residual $BaCO_3$ and $SrCO_3$ contained in the precursor mixtures. The nascent BaO could have reacted shortly afterwards with other components of the mixtures to form additional amounts of Hexacelsian and Celsian. The chemical reactions likely occurring in the temperature ranges just mentioned were deduced based on observations previously reported by Long-González et al. (14) and Maitra and Foger (33). The relative importance of the last region decreased appreciably with increasing milling time as well as with decreasing $BaCO_3$ and $SrCO_3$ content in the precursor mixtures, in such a way that it disappears completely for composition 1 milled for 8 h, as well as for compositions 2 and 3 milled either for 4 h or 8 h. This suggests that in all these cases both carbonates had been almost completely consumed in the materials at < 900 °C. Lastly, apparently $SrCO_3$ participated only in the formation of the SBAS solid solution in the temperature range of ~700-1500 °C, at which there was also a likely formation of a certain amount of transient liquid in the materials. The grounds that support the latter assumptions will be discussed further in section 3.2.

3.2. Phase composition of green and sintered materials

The XRD patterns (not shown) obtained for all the green samples, with or without mechanical activation, revealed only the presence of the original raw materials ($BaCO_3$, $SrCO_3$, Al_2O_3, ZrO_2, and α-quartz contained in the FA). It was also observed that the reflections of all detected crystalline phases tended to become broader and less intense with increasing milling time, which was associated with a small loss of their crystallinity as a consequence of mechanical activation.

In all cases, only four crystalline phases (Celsian, Hexacelsian, t-ZrO_2 and m-ZrO_2) were detected by XRD in the sintered samples (Figure 2). The formation of barium-containing transient phases was not detected in any of our sintered materials. However, based on the related published literature, the formation of this kind of compounds was not ruled out in this work. Long-González et al. (14) detected the presence of Hexacelsian, Al_2O_3, $BaAl_2O_4$, $BaSiO_3$, Ba_2SiO_4, $BaSi_2O_5$, and traces of $BaCO_3$, after reactive sintering at 900 °C / 5 h of a non-mechanically activated precursor mixture prepared using the same raw materials employed by us, but without the addition of ZrO_2. In this work, transient compounds such as the ones just mentioned were presumably formed and subsequently fully consumed during the formation of SBAS (Hexacelsian and/or Celsian) at temperatures below 900 °C. Thus, in our case the solid state reactions were presumably faster and took place at temperatures lower than 900 °C, which was probably caused by mechanical activation of our materials combined with the presence of ZrO_2 and a likely generation in them of considerable amounts of transient liquid during the sintering stage. Our XRD results also suggested that $SrCO_3$ participated only in the formation of the SBAS solid solution in the temperature range of ~700-1500 °C, since no additional SrO-containing phases were formed in this temperature range. This was further supported by the

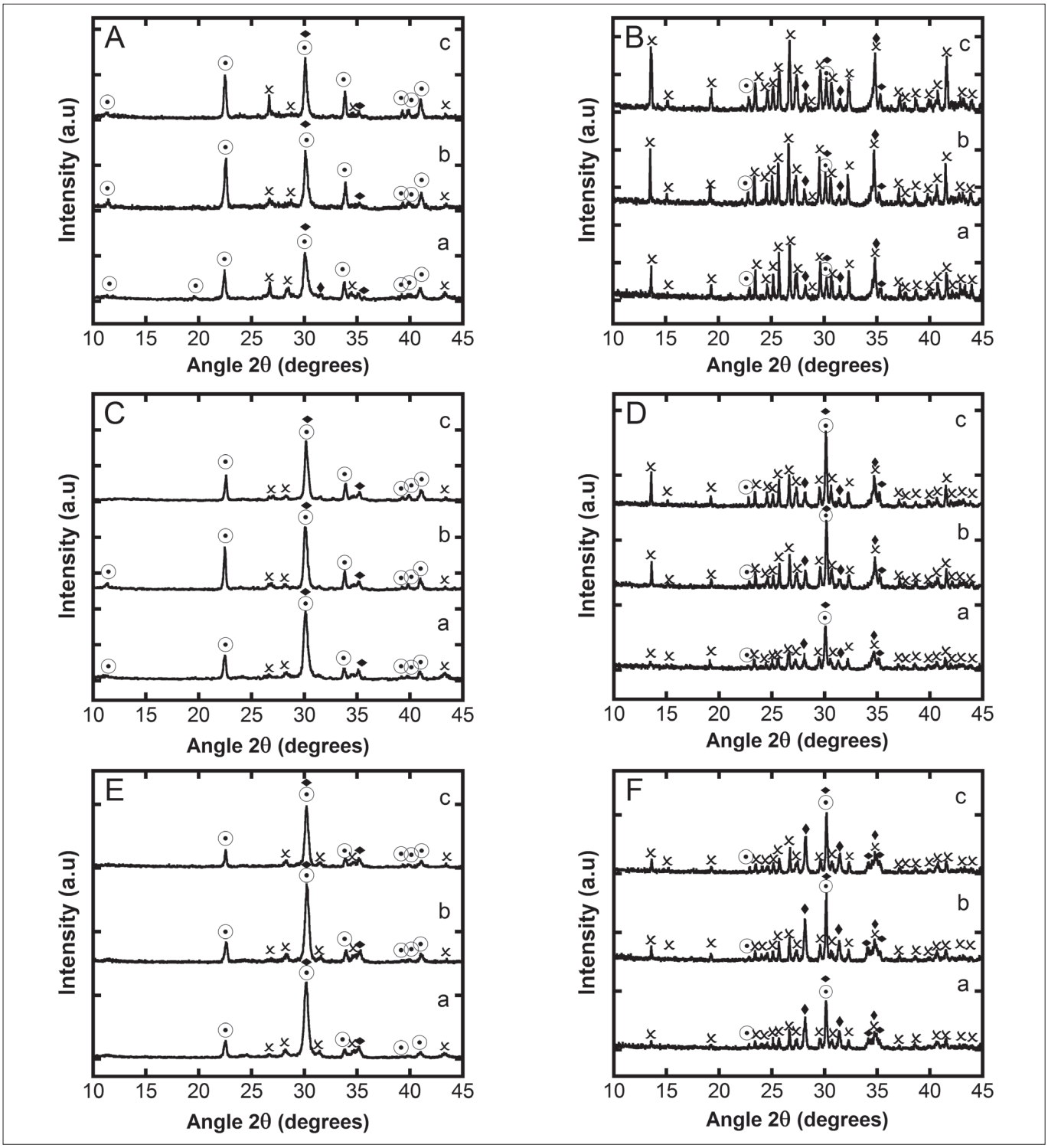

Figure 2. XRD patterns of compositions 1 (A,B), 2 (C,D) and 3 (E,F), milled for: a) 0 h, b) 4 h and c) 8 h, and then sintered at either 900 °C (A,C,E) or 1500 °C (B,D,F). Key: ✗ Celsian, ⊙ Hexacelsian, ⬥ m-ZrO_2, and ⬥t-ZrO_2.

results previously reported by some of the present authors (14). Lastly, the formation of solid solutions of ZrO_2 in SBAS, as reported by Sandhage and Fraser (6), and Debsikdar and Sowemimo (7), was not detected in this work.

According to Figure 3, some marked variations with respect to the nominal relative proportions were observed in the SBAS and ZrO_2 phases detected by XRD in the sintered samples. This caused the disagreement indicated in Table III between the experimental and the nominal SBAS/ZrO_2 mass ratios. In the case of composition 1, this was probably due to a lack of completeness of the crystallization of SBAS at 900 °C, independently of milling time, from a small proportion of a transient glassy phase likely formed in the samples under those conditions. This in turn caused that the relative proportion of SBAS was lower and that of ZrO_2 was higher, with respect to the nominal values. Once the sintering temperature was increased, additional amounts of SBAS were formed by crystallization of the transitory glassy phase present in the

Bol. Soc. Esp. Ceram. Vidr. Vol 53. 4, 179-193, Julio-Agosto 2014. ISSN 0366-3175. eISSN 2173-0431. http://dx.doi.org/10.3989/cyv.222014

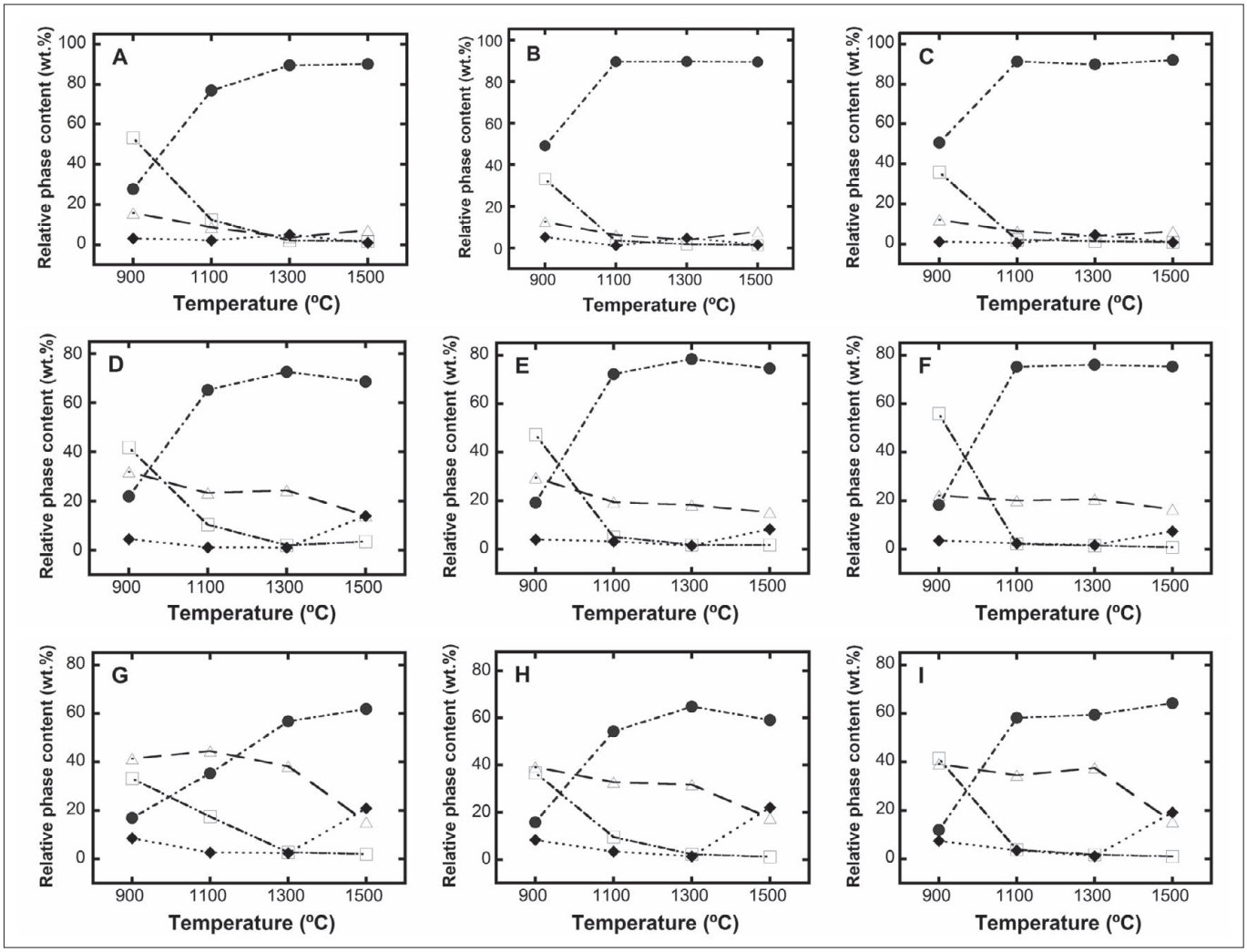

Figure 3. Phase evolution for compositions 1 (A,B,C), 2 (D,E,F) and 3 (G,H,I), as a function of sintering temperature, without mechanical activation (A,D,G) or milled either for 4 h (B,E,H) or 8 h (C,F,I). Key: ♦ m-ZrO_2, Δ t-ZrO_2, ● Celsian, and □ Hexacelsian. The standard error estimated for these determinations was ±5 %.

TABLE III. EXPERIMENTAL SBAS/ZrO_2 WEIGHT RATIOS OBTAINED AS A FUNCTION OF MILLING TIME (H) AND SINTERING TEMPERATURE FOR THE STUDIED COMPOSITIONS. THE CORRESPONDING NOMINAL SBAS/ZrO_2 MASS RATIOS ARE SHOWN INSIDE THE PARENTHESES. EXPERIMENTAL VALUES RELATIVELY CLOSE TO THE NOMINAL ONES ARE WRITTEN IN BOLD AND ITALICS. KEY: SBAS = WT. % CELSIAN + WT. % HEXACELSIAN; ZrO_2 = WT. % T-ZrO_2 + WT. % M-ZrO_2.

Sintering Temperature (°C)	Composition 1 (90/10)			Composition 2 (70/30)			Composition 3 (50/50)		
	0	4	8	0	4	8	0	4	8
900	81/19	86.7/13.3	82.1/17.8	63.7/36.3	66.5/33.5	***74.2/25.8***	***50.1/49.9***	***52.5/47.5***	***53.4/46.7***
1100	***89.3/10.8***	***92.9/7.4***	***93.3/6.8***	***75.6/24.4***	77.3/22.7	77.5/22.5	***52.8/47.2***	63.8/36.2	61.9/38.1
1300	***91.5/8.5***	***91.3/8.7***	***91.3/8.7***	***74.6/25.4***	80.2/19.8	77.6/22.3	59.5/40.6	67.1/32.9	61.2/38.7
1500	***91.8/8.2***	***90.7/9.3***	***93/7***	***72.1/27.9***	76.4/23.6	76.1/23.9	63.8/36.2	60.3/39.7	65.3/34.7

samples. As a result, the relative proportion of SBAS increased and that of ZrO_2 decreased, and the composition of the materials became closer to the nominal one. It is thought that a similar phenomenon took place in the case of composition 2, either without mechanical activation or milled for 4 h and subsequently sintered at 900 °C. In the rest of the samples of compositions 2 and 3 whose experimental compositions disagreed with the nominal one, the concentration of SBAS tended to be higher and that of ZrO_2 tended to be lower, with respect to the nominal values. This could be attributed to a partial dissolution of t-ZrO_2 in a transient liquid formed in the materials during the sintering process, and this dissolution increased proportionally with increasing sintering temperature. This was followed by re-precipitation of some m-ZrO_2 from the transient liquid at temperatures ≥1300 °C, when the liquid became saturated in ZrO_2 due to the consumption of a considerable portion of its content of BaO, SrO, Al_2O_3 and SiO_2 for the formation of additional amounts of SBAS in the materials. This suggests that some of the Y_2O_3 that was originally contained in the 3 mol. % Y_2O_3-stabilized

ZrO_2 employed by us remained dissolved in the remnant transient liquid, and then it probably remained dissolved in a glassy phase likely originated from that liquid during cooling of the samples, which was probably not detected by XRD due to its small amount. Consequently, not enough Y_2O_3 remained in solid solution in the re-precipitated ZrO_2 to ensure its full stabilization into the tetragonal form (10,34).

The previous discussion relies on the assumption that all compositions studied in this work had a considerable tendency towards the formation of transient liquid during the sintering process, and that this tendency was accentuated by mechanical activation of the materials. This assumption was based on an analysis of the pertinent published literature, but it was not experimentally verified. It is well-known (35) that some of the impurities contained in the FA, such as alkaline metal oxides (Na_2O and K_2O), alkaline-earth metal oxides (CaO and MgO), and iron oxides, can act as fluxes that promote the formation of a great deal of liquid in the materials at high temperatures. The presence of large proportions of $BaCO_3$ and $SrCO_3$ increased even more the fluxing effect on the FA and on other components of the precursor mixtures (36,37), especially in the case of composition 1. Furthermore, the diffusion of BaO and SrO into the structure of the aluminosilicates present in the FA could lead to the formation of additional amounts of amorphous phases (38), which in turn could be easily melted at high temperatures, especially in the presence of a large amount of fluxing agents. Since it is very likely that the transient liquid had high contents of BaO and SrO, this would give it a capability to dissolve considerable amounts of ZrO_2 (39). Besides, Y_2O_3-stabilized ZrO_2 is more prone to be dissolved by corrosive liquids, in comparison with pure ZrO_2 (40). Lastly, the generation of further amounts of transient liquid could be caused by the likely formation of a pseudo-eutectic at relatively low temperatures as a result of the combination of ZrO_2 with $BaCO_3$, $SrCO_3$ and the impurities present in the FA (Na_2O, K_2O, CaO, MgO and iron oxides) (41).

3.3. Microstructural evolution in the sintered materials

For all compositions and milling times employed, it was observed, see Figures 4 and 5 (a,c,e), that in general the materials sintered at 900 °C showed a poorly densified microstructure. This was probably due to the generation of transient liquid during the sintering process, but in an amount insufficient to produce a high degree of consolidation in the materials, leading to the presence in them of a residual glassy phase (10). Obviously, this temperature was also too low to produce a good sintering degree in the samples.

In contrast, according to Figures 4 and 5 (b,d,f), for all three studied compositions sintered at 1500 °C, we observed a well-defined microstructure constituted by two phases: a grey SBAS (Hexacelsian + Celsian) matrix plus a considerable number of small and globular white ZrO_2 particles scattered all over the SBAS matrix. These phases were identified with the aid of the corresponding EDS spectra (Figure 6). The globular morphology of the ZrO_2 particles was typical of a phase which was formed in the presence of transient liquid. This phenomenon was also observed by Nordmann et al. (10), and it is very similar to that seen during corrosion of Y_2O_3-stabilized ZrO_2 by molten glasses of the CMAS (CaO-MgO-Al_2O_3-SiO_2) system (42-45). ZrO_2 was found as isolated particles with sizes ≤ 1μm as well as forming clusters with sizes ≤ 15μm. In all cases, with increasing milling time, the size of the ZrO_2 particles tended to increase by coalescence, and also became better distributed in the materials' microstructure.

Lastly, in all cases a large number of microcracks was observed in the SBAS matrix, which could be attributed mainly to a mismatch existing between the CTE of Hexacelsian, Celsian, t-ZrO_2 and m-ZrO_2 present in our materials. It has been suggested (9) that this microcracking could improve the thermal shock resistance of the BAS-ZrO_2 composite materials, but this hypothesis was not verified in this work.

These results are comparable with those of Nordlie (9), who found that the development of Celsian and Zirconia phases in BAS-ZrO_2 composites required treating their precursor mixtures at least at 1400 °C/6 h. Similarly, Nordmann et al. (10) also concluded that it is possible to obtain a dispersion of ZrO_2 particles in a BAS matrix above 1400 °C.

3.4. Hexacelsian to Celsian conversion fraction (*f*)

As it can be seen in Figure 7, in all the studied compositions *f* increased with increasing sintering temperature and milling time, especially in the temperature range of 900-1100 °C. In the temperature range of 1300-1500 °C, all materials achieved *f* values very close to 100 %, especially in the case of compositions 1 and 2, and these values were nearly constant and independent of milling time. It was observed that the temperature range at which such high *f* values were obtained could be broaden to 1100-1500°C, with the aid of mechanical activation of the precursor mixtures. This was achieved in the case of compositions 1 and 2 mechanically activated for at least 4 h, especially in the former material. However, in the case of composition 3 the same goal could be achieved only after 8 h of milling. It was also observed that in the temperature range of 900-1100 °C, for a given milling time, the value of *f* decreased with increasing content of ZrO_2 in the materials. Similarly, although a value of *f* very close to 100 % was reached in all cases with a sintering temperature of 1500 °C, independently of milling time, the value of *f* tended to decrease with increasing ZrO_2 content in the composites. In this way, the mean *f* values obtained for the materials sintered at the latter temperature, when averaged over all milling times employed, were ~98 % for compositions 1 and 2, and ~97 % for composition 3. Thus, although in this work Hexacelsian to Celsian conversions very close to 100 % were obtained under certain experimental conditions, a full conversion was never attained in any of our compositions, which could be due to the presence of ZrO_2 in them, since this oxide tends to favor the formation of Hexacelsian.

The latter results indicate that ZrO_2 decreases the Hexacelsian to Celsian conversion in the composites, and this effect becomes more pronounced with increasing content of this oxide in the materials. However, in order to obtain a value of *f* close to 100 % at a sintering temperature of 1100 °C, the deleterious effect of ZrO_2 could be nearly overcome if a sufficiently long mechanical activation is given to the precursor mixtures, whose required duration is directly proportional to the content of ZrO_2 in the materials.

Other researchers obtained Hexacelsian to Celsian conversion fractions similar to those obtained by us, although for BAS-ZrO_2 composites and employing multi-step processes, as well as higher temperatures and/or longer thermal treatments. For instance, Sandhage and Fraser (6) obtained

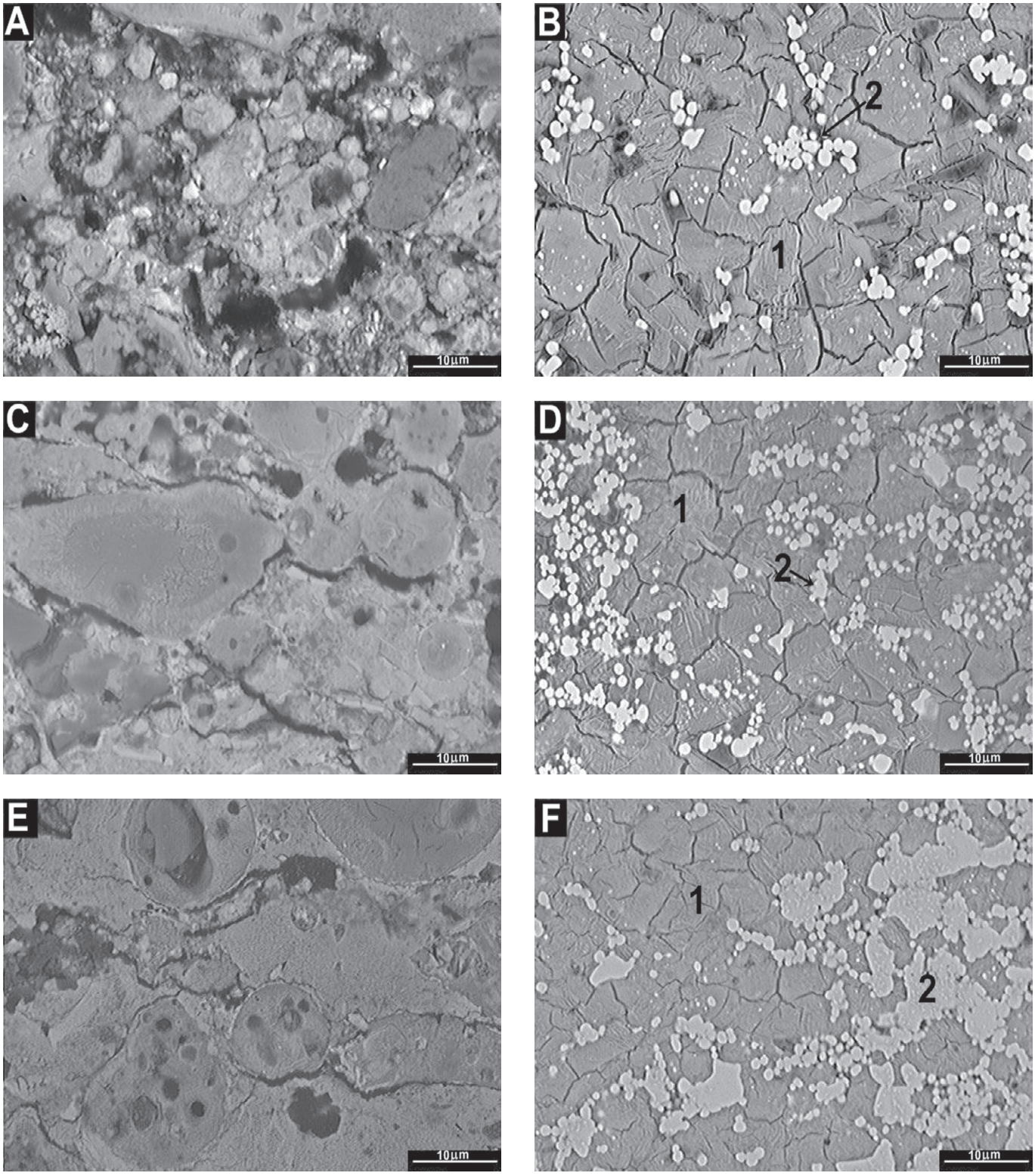

Figure 4. SEM micrographs of compositions 1 (a,b), 2 (c,d) and 3 (e,f), without mechanical activation and sintered at either 900 °C (a,c,e) or 1500 °C (b,d,f). Key: 1) SBAS and 2) ZrO_2.

Celsian and m-ZrO_2 in BAS-ZrO_2 composites synthesized at 1200 °C/26 h using the so-called "oxidation of solid metal-bearing precursors (SMP)" method. Debsikdar and Sowemimo (7) obtained Celsian ceramics by sintering cold isostatically pressed pellets at 1450 or 1580 °C, apparently for 20 h in both cases, which were produced from BAS powder mixtures containing 20 wt. % gel-derived lithia-doped Celsian seed powder to promote the Hexacelsian to Celsian transformation during sintering plus 7.6 or 18 wt. % t-ZrO_2. Nordlie (9) obtained Celsian in BAS-ZrO_2 composites containing 30-60 wt. % ZrO_2 when these were first fired at 1410 °C/6 h, and then re-fired at 1650 °C/6 h. Lastly, Nordmann et al. (10) were unable to obtain Celsian in BAS-ZrO_2 composites containing ~25-40 wt. % ZrO_2 (with the balance BAS plus 0-5 wt. % Y_2O_3

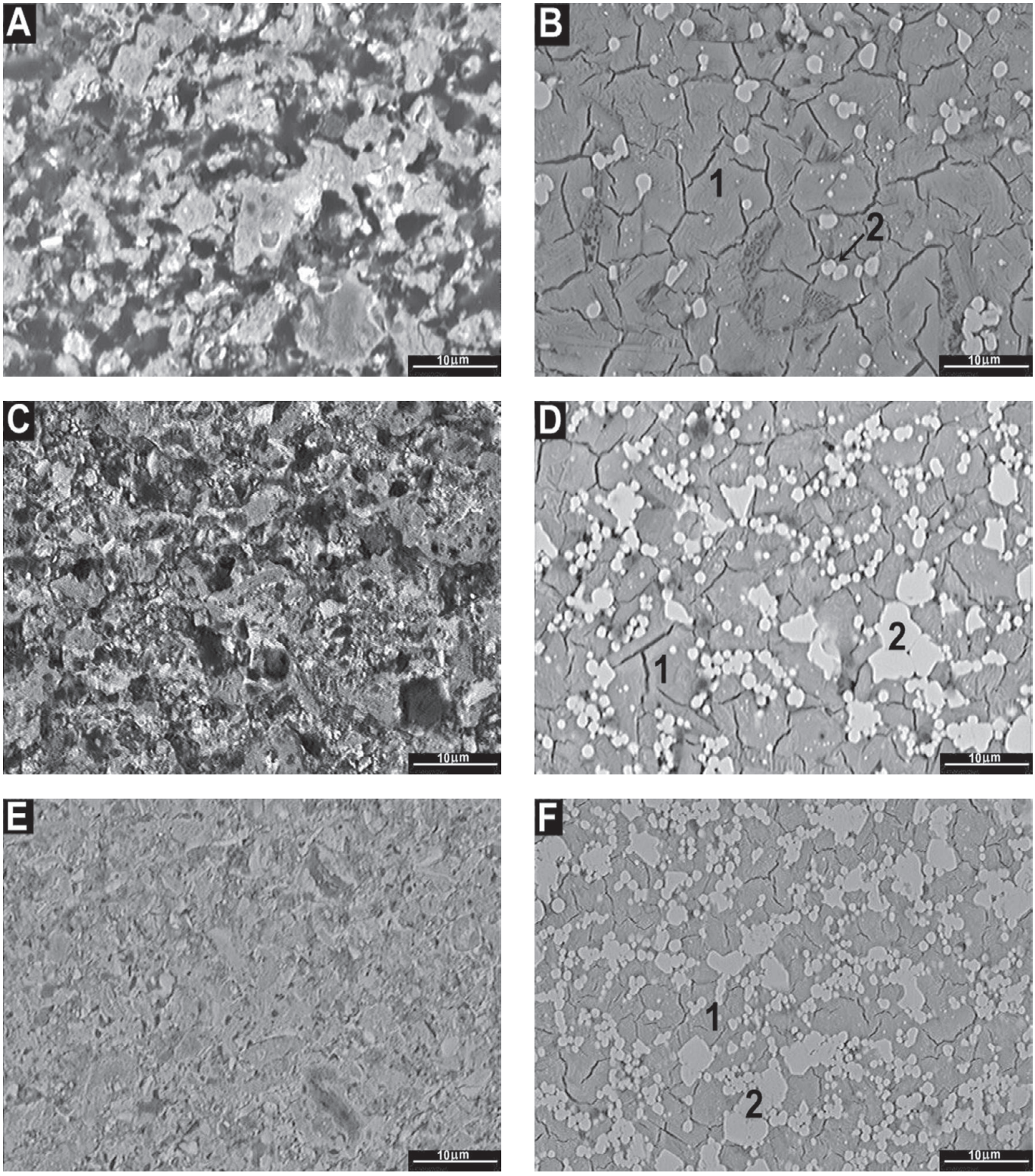

Figure 5. SEM micrographs of compositions 1 (a,b), 2 (c,d) and 3 (e,f), mechanically activated for 8 h and sintered at either 900 °C (a,c,e) or 1500 °C (b,d,f). Key: 1) SBAS and 2) ZrO_2.

added for the stabilization of t-ZrO_2), which were synthesized at 1000-1600 °C/2 h without the addition of mineralizing agents.

In this work, it was possible to obtain Hexacelsian to Celsian conversions close to 100 % at a sintering temperature as low as 1100 °C, using a simple one-step sintering process, not only due to our use of mechanical activation as a pre-treatment for our precursor mixtures, but also due to our use of SBAS instead of BAS, as well as due to our use of FA as one of the main raw materials for the synthesis of the composites, since it has been observed (14) that some of the FA impurities (Na_2O, CaO, TiO_2 and MgO) could act as mineralizers that enhance the Hexacelsian to Celsian conversion in the materials.

Bol. Soc. Esp. Ceram. Vidr. Vol 53. 4, 179-193, Julio-Agosto 2014. ISSN 0366-3175. eISSN 2173-0431. http://dx.doi.org/10.3989/cyv.222014

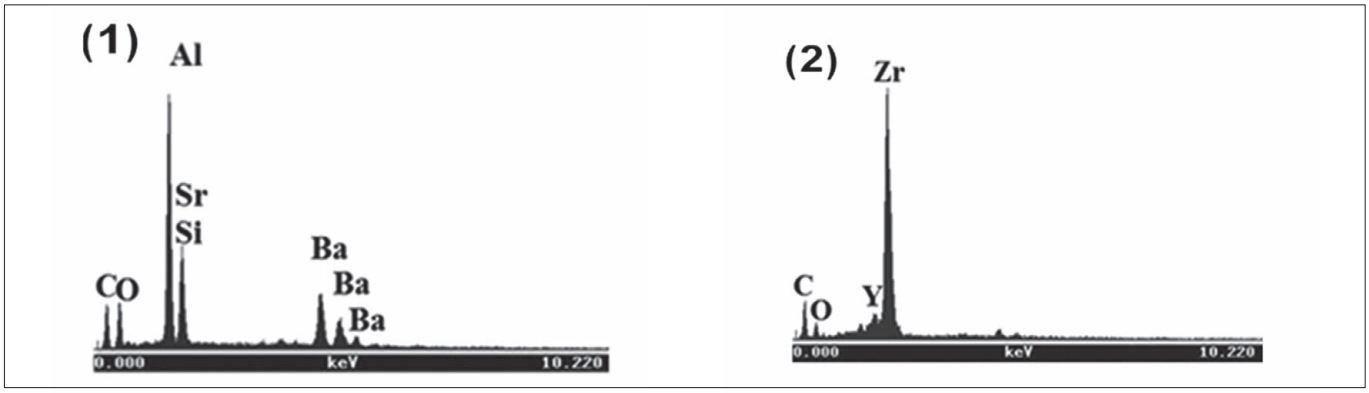

Figure 6. Typical EDS spectra obtained for the phases observed on the SEM micrographs. Key: 1) SBAS and 2) ZrO_2 phases.

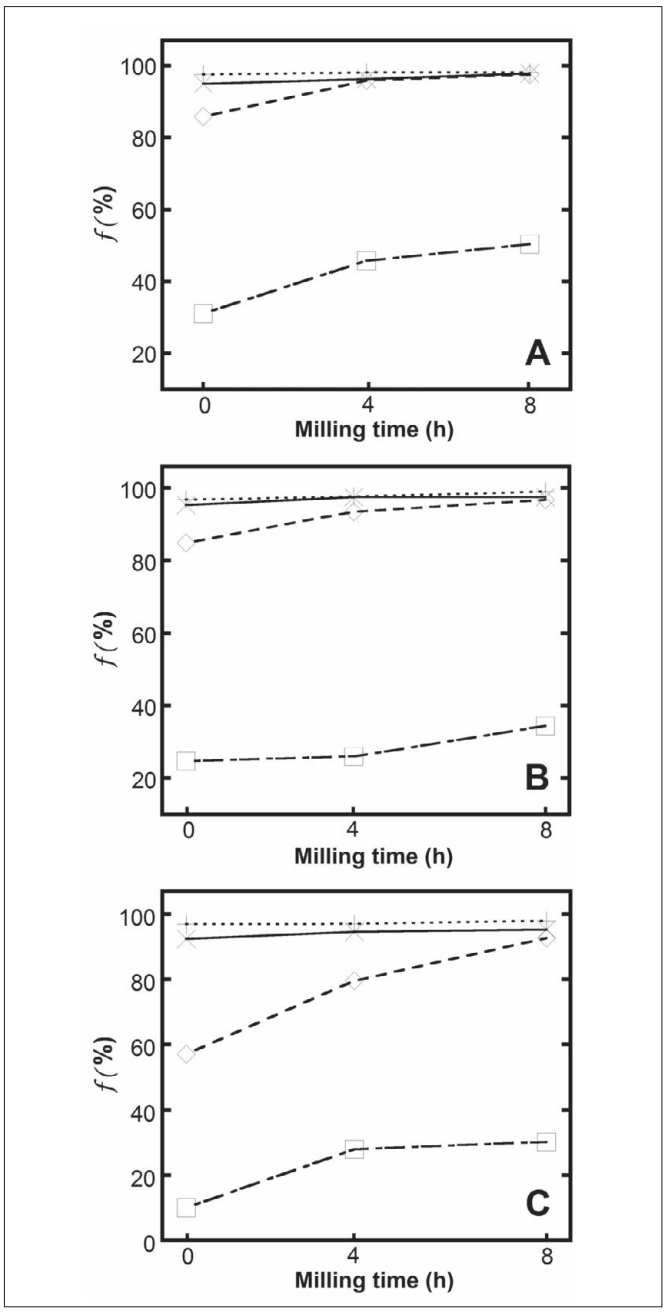

Figure 7. Hexacelsian to Celsian conversion fraction (*f*) as a function of milling time for compositions 1 (A), 2 (B), and 3 (C), sintered at 900 ºC (□), 1100 ºC (◇), 1300 ºC (X), and 1500 ºC (+). The standard error estimated for these determinations was ±5 %.

In summary, in terms of the Hexacelsian to Celsian conversion, we were interested in achieving a value of it as close to 100 % as possible, even for compositions with relatively high contents of ZrO_2, for the reasons already explained. In this sense, our results showed that at sintering temperatures below 1300 °C the most important factor was the combined use of mechanical activation plus FA and SBAS contained in the materials. This allowed us to achieve conversion values very close to 100 % at these sintering temperatures with increasing milling time, even for the case of materials containing considerable proportions of ZrO_2 in their composition. Thus, at these sintering temperatures a synergistic effect took place between the FA and the SBAS present in the materials and the mechanical activation given to the latter, in such a way that the Hexacelsian to Celsian conversion was in fact promoted by an increment in the milling time, in contrast with previous results reported in the literature (13). However, in order to achieve high conversion values, the milling time had to be increased in a directly proportional manner with respect to the increment in the ZrO_2 content of the materials. On the other hand, in the temperature range of 1300-1500 °C, the most important factor was the sintering temperature. In this temperature range, all compositions tended to achieve conversion values very close to 100 %, independently of milling time, which was more accentuated for the case of compositions 1 and 2, which had the smallest contents of ZrO_2.

3.5. Evaluation of physical properties of sintered materials

3.5.1 RELATIVE DENSITY

As it can be seen in Figure 8, in general the relative density of the composite materials tended to increase with increasing sintering temperature and with increasing milling time. It can be noticed that in all cases the maximum relative density was achieved at a sintering temperature of 1500 °C, for a milling time whose duration decreased with decreasing content of ZrO_2 in the precursor mixtures. At a sintering temperature of 1500 °C, it was observed that composition 1 showed a constant relative density, very close to 1, independently of milling time, while compositions 2 and 3 achieved similarly high relative densities for milling times of at least 4 h in the first case, and of at least 8 h in the second case. These results suggest that with increasing ZrO_2 content, an increased in both the milling time and the sintering temperature was required in order to obtain a high degree of densification in the composite materials.

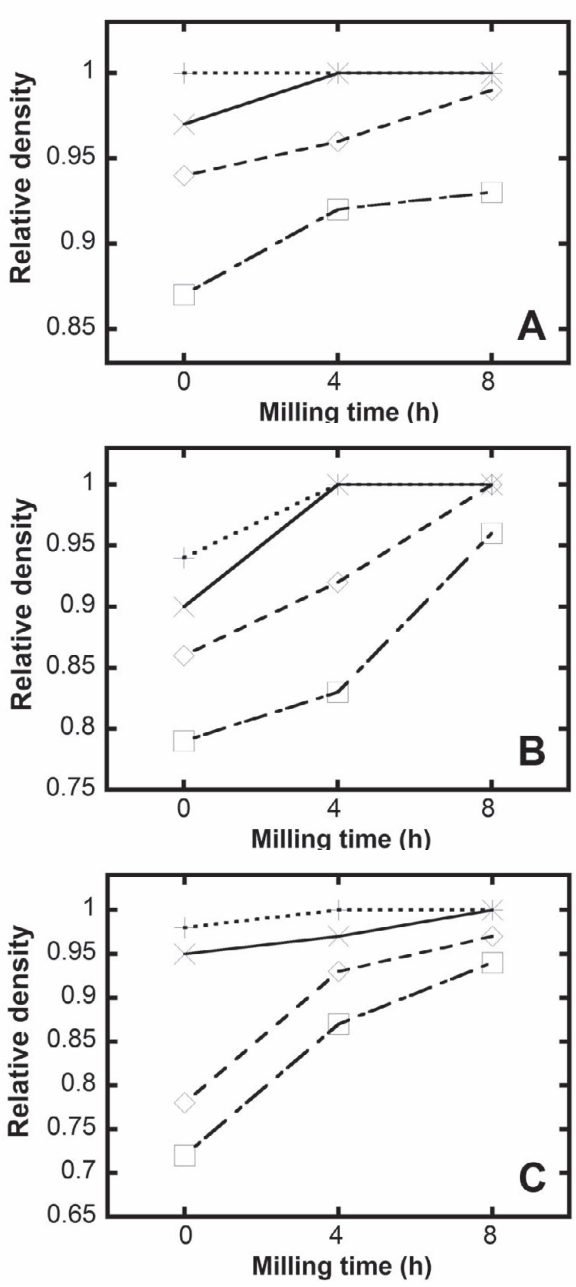

Figure 8. Relative density of compositions 1 (A), 2 (B), and 3 (C), sintered at 900 ºC (□), 1100 ºC (◇), 1300 ºC (X), and 1500 ºC (+).

Our results compare favorably with those previously reported. For instance, Debsikdar and Sowemimo (7) obtained relative densities of 95 % and 99 % for their materials described in the previous section of this paper. Nordmann et al. (10) observed a significant increase in the rate of densification above 1300 °C, obtaining a maximum density of 3.52 g/cm^3 for a binary BAS-ZrO_2 composition containing ~40 wt. % ZrO_2 and sintered at 1500 °C/2 h. This was attributed to the generation of transient liquid which started at 1300 °C, and which facilitated the densification of the material.

3.5.2 COEFFICIENT OF THERMAL EXPANSION (CTE)

The CTE was not evaluated in the samples sintered at 900 °C, due to their poor mechanical properties. Table IV shows the values of CTE obtained from room temperature up to 1300 °C for all the studied compositions as a function of milling time and sintering temperature. As it can be seen, the CTE tended to decrease with increasing sintering temperature, milling time and nominal content of SBAS in the composite compositions. This was probably related to the fact that Celsian prevailed over Hexacelsian in those compositions, as well as to the fact that the CTE of the latter phases are considerably lower than that of ZrO_2 (9). In this way, the smallest CTE value (4.79 x 10^{-6} °C^{-1}) was obtained for composition 1 milled for 8 h and sintered at 1500 °C.

TABLE IV. VALUES OF CTE (x10^{-6} °C^{-1}) OBTAINED FOR THE STUDIED COMPOSITIONS.

Composition	Milling time (h)	Sintering temperature (°C)		
		1100	1300	1500
1	0	6.45	6.17	5.74
	4	5.71	5.64	5.40
	8	5.22	5.07	4.79
2	0	6.56	6.21	5.93
	4	6.19	5.65	5.40
	8	5.43	5.26	5.18
3	0	7.30	7.15	6.97
	4	6.72	6.65	6.59
	8	6.68	6.10	5.43

Our results are comparable with those reported by Nordlie (9). This author observed that the CTE gradually diminished with increasing BAS content in BAS-ZrO_2 composites containing 40-70 wt. % BAS in which Celsian prevailed, from a value of 5.05x10^{-6} °C^{-1} for the material containing 43 wt. % BAS to a value of 4.0x10^{-6} °C^{-1} for the material with 64 wt. % BAS, in the temperature range from room temperature to 1000 °C.

3.6. Evaluation of mechanical properties of sintered materials

Similarly to the observations recently reported by the present authors for the case of SBAS-Al_2O_3 composites (17), all the evaluated mechanical properties of the materials synthesized in this work increased with increasing milling time, sintering temperature and ZrO_2 content. Thus, the best mechanical properties were obtained for composition 3 milled for 8 h and sintered at 1500 °C. This could be related to the fact that ZrO_2, like Al_2O_3, also has better mechanical properties than SBAS. On the other hand, in the case of all compositions milled for 8 h and sintered at 1500 °C, the better distribution achieved by the ZrO_2 particles in a predominantly Celsian matrix, together with the high degree of consolidation achieved by the samples synthesized under these conditions, could lead to a better distribution of the applied stresses between the matrix and the reinforcement phase in the ceramic composites, which resulted in the attainment of the best mechanical properties in the latter materials.

3.6.1 YOUNG'S MODULUS

According to Table V, except for a few cases, the values of the Young's modulus (E) that were obtained by four-point flexural strength tests tended to be lower than those determined by using the ultrasonic technique. The few instances in which this was not the case could be explained based on the fact that the

TABLE V. VALUES OF YOUNG'S MODULUS (GPA) OBTAINED FOR THE STUDIED COMPOSITIONS AS A FUNCTION OF MILLING TIME AND SINTERING TEMPERATURE. THE STANDARD ERROR IS GIVEN FOR ALL THE REPORTED MEASUREMENTS. KEY: E(U) = YOUNG'S MODULUS DETERMINED BY ULTRASONIC TECHNIQUE, AND E(MT) = YOUNG'S MODULUS DETERMINED BY MECHANICAL TESTING.

Composition	Milling time (h)	Sintering temperature (°C)					
		1100		1300		1500	
		E (U)	E (MT)	E (U)	E (MT)	E (U)	E (MT)
1	0	7.00 ± 1.47	4.56 ±2.71	8.85 ± 6.77	6.65 ± 3.55	10.97 ± 0.35	9.11 ± 2.71
	4	10.04 ± 3.68	6.70 ± 2.87	18.35 ± 3.18	15.45 ± 2.01	28.80 ± 1.20	20.30 ± 1.31
	8	12.45 ± 1.20	11.38 ± 1.23	19.97 ± 1.56	17.43 ± 1.15	43.12 ± 4.73	29.22 ± 0.80
2	0	7.82 ± 1.30	6.48 ± 2.57	7.96 ± 6.80	7.90 ± 1.70	8.28 ± 1.27	7.24 ± 2.09
	4	10.23 ± 0.92	9.13 ± 0.72	10.89 ± 5.94	11.28 ± 2.84	12.45 ± 0.50	10.42 ± 4.39
	8	13.39 ± 2.58	12.20 ± 0.71	14.38 ± 3.29	13.14 ± 0.08	36.65 ± 4.85	30.57 ± 1.25
3	0	7.89 ± 3.75	7.67 ± 2.30	9.16 ± 0.71	11.81 ± 1.49	10.10 ± 0.92	9.41 ± 0.63
	4	8.32 ± 5.54	11.18 ± 1.50	10.19 ± 0.99	13.36 ± 1.45	20.08 ± 3.03	18.97 ± 1.73
	8	14.75 ± 4.99	13.79 ± 1.29	28.37 ± 2.62	23.17 ± 1.56	48.79 ± 0.71	32.14 ± 1.97

TABLE VI. VALUES OF THE MODULUS OF RUPTURE (MOR, MPA) DETERMINED FOR THE STUDIED COMPOSITIONS AS A FUNCTION OF MILLING TIME AND SINTERING TEMPERATURE. THE STANDARD ERROR IS GIVEN FOR ALL THE REPORTED MEASUREMENTS.

Composition	Milling time (h)	Sintering temperature (°C)		
		1100	1300	1500
1	0	11.41 ± 0.46	12.43 ± 0.82	15.95 ± 2.20
	4	12.37 ± 0.57	14.39 ± 1.05	16.43 ± 0.25
	8	18.51 ± 0.39	19.00 ± 0.08	20.71 ± 0.16
2	0	4.36 ± 0.67	5.82 ± 0. 42	6.75 ± 0.39
	4	5.88 ± 0.30	6.29 ± 0.51	7.44 ± 0.81
	8	6.38 ± 0.29	7.53 ± 0.55	21.40 ± 4.18
3	0	4.23 ± 0.63	8.39 ± 0.39	9.16 ± 0.13
	4	6.55 ± 0.32	9.55 ± 0.17	13.17 ± 0.05
	8	9.54 ± 0.41	10.20 ± 0.41	21.75 ± 0.30

TABLE VII. FRACTURE TOUGHNESS (K_{IC}, $MPa \bullet m^{1/2}$) DETERMINED FOR THE STUDIED COMPOSITIONS AS A FUNCTION OF MILLING TIME AND SINTERING TEMPERATURE. THE STANDARD ERROR IS GIVEN FOR ALL THE REPORTED MEASUREMENTS.

Composition	Milling time (h)	Sintering temperature (°C)		
		1100	1300	1500
1	0	0.28 ± 0.004	0.35 ± 0.009	0.45 ± 0.02
	4	0.31 ± 0.04	0.36 ± 0.02	0.48 ± 0.03
	8	0.54 ± 0.02	0.53 ± 0.02	0.77 ± 0.004
2	0	0.65 ± 0.02	1.15 ± 0.01	2.17 ± 0.02
	4	1.02 ± 0.02	1.63 ± 0.03	2.40 ± 0.04
	8	1.25 ± 0.01	1.74 ± 0.009	2.66 ± 0.009
3	0	0.39 ± 0.004	0.45 ± 0.01	2.14 ± 0.02
	4	1.39 ± 0.03	1.47 ± 0.004	2.42 ± 0.04
	8	1.51 ± 0.01	1.87 ± 0.04	2.78 ± 0.01

ultrasonic method does not take into account the distribution of defects in the materials. Composition 3 milled for 8 h and sintered at 1500 °C achieved maximum values of 48.79 ± 0.71 GPa, according to the ultrasonic technique, and of 32.14 ± 1.97 GPa, according to the four-point flexural strength tests.

3.6.2 MODULUS OF RUPTURE (MOR)

The measured MOR values are shown in Table VI. The maximum MOR value obtained was 21.75 ± 0.30 MPa, which corresponded to composition 3 milled for 8 h and sintered at 1500 °C. This value is comparable with the ones reported by Nordlie (9) for Celsian-ZrO_2 compositions fired in an electric furnace at 1420 °C/6 h and then re-fired in a gas kiln at 1650 °C/6 h. These authors claimed that their results were rather uniform, obtaining a mean MOR value of ~27.6 MPa for all their studied compositions. However, they also reported that a minimum MOR value of ~18-25 MPa was obtained for their compositions containing 40-70 wt. % Celsian, possibly due to

TABLE VIII. VICKERS MICROHARDNESS (HV, KG/MM^2) DETERMINED FOR THE STUDIED COMPOSITIONS AS A FUNCTION OF MILLING TIME AND SINTERING TEMPERATURE. THE STANDARD ERROR IS GIVEN FOR ALL THE REPORTED MEASUREMENTS.

Composition	Milling time (h)	Sintering temperature (°C)		
		1100	1300	1500
1	0	4.90 ± 0.63	89.47 ± 2.37	217.07 ± 5.36
	4	10.16 ± 0.17	151.23 ± 1.27	422.92 ± 0.97
	8	128.20 ± 4.92	281.53 ± 5.72	493.32 ± 6.72
2	0	8.85 ± 0.74	165.66 ± 6.05	227.96 ± 5.04
	4	43.07 ± 2.12	341.45 ± 3.48	601.75 ± 4.77
	8	290.03 ± 5.75	511.39 ± 2.54	713.74 ± 5.91
3	0	9.36 ± 5.75	147.79 ± 3.11	351.90 ± 0.92
	4	201.43 ± 5.11	481.82 ± 3.70	415.79 ± 1.42
	8	288.52 ± 1.07	642.42 ± 2.85	772.58 ± 5.74

the formation of a higher concentration of microcracks in them caused by their relatively higher Celsian content.

3.6.3 FRACTURE TOUGHNESS (K_{IC})

The values of K_{IC} obtained for the sintered materials are shown in Table VII. A maximum K_{IC} value of 2.78 ± 0.01 MPa•m$^{1/2}$ was obtained for composition 3 milled for 8 h and sintered at 1500 °C.

3.6.4 VICKERS MICROHARDNESS (HV)

The values determined for the Vickers microhardness (HV) are given in Table VIII. A maximum HV value of 772.58 ± 5.74 Kg/mm^2 was obtained for composition 3 milled for 8 h and sintered at 1500 °C. This value was lower than the 1101 Kg/mm^2 reported by Debsikdar and Sowemimo (7) for 99 % dense Celsian ceramic with the addition of 20 mol. % t-ZrO_2 and sintered at 1580 °C/2 h. In our work, in many cases ZrO_2 was present in the sintered materials mainly in its monoclinic form, and this could be associated with the lower HV values obtained by us.

4. CONCLUSIONS

The reactivity of the precursor mixtures was enhanced by mechanical activation combined with the likely generation of a considerable amount of transient liquid during sintering of the materials. ZrO_2 decreased the Hexacelsian to Celsian conversion, which was more pronounced when its content was increased in the composites. Nearly full Hexacelsian to Celsian conversions could be achieved at a sintering temperature as low as 1100 °C, by mechanically activating the precursor mixtures for a time that increased with increasing content of ZrO_2 in the materials. The dissolution/re-precipitation of ZrO_2 in the formed transient liquid caused certain degree of disagreement between the experimental and the nominal composite compositions, especially in the materials with the highest ZrO_2 contents, which were mechanically activated for either 4 h or 8 h, and sintered above 900 °C. All the evaluated mechanical properties increased with increasing time of mechanical activation, sintering temperature and ZrO_2 content in the ceramic composites. In this way, the best results were obtained for composition 3 milled for 8 h and sintered at 1500 °C, which were: E(U) = 48.79 ± 0.71 GPa, E(MT) = 32.14 ± 1.97 GPa, MOR = 21.75 ± 0.30 MPa, K_{IC} = 2.78 ± 0.01 MPa•m$^{1/2}$, and HV = 772.58 ± 5.74 Kg/mm^2.

ACKNOWLEDGEMENTS

The authors express their gratitude to CONACYT and Cinvestav-Saltillo for the financial support and experimental facilities provided for the development of this work. Many thanks are also given to the personnel of the "José López Portillo" power plant, Nava, Coahuila, México, for supplying the employed FA.

REFERENCES

1. Zhang, X. -D.; Sandhager, K. H.; Fraser, H.L.; (2005): Synthesis of $BaAl_2Si_2O_8$ from solid Ba-Al-Al_2O_3-SiO_2 precursors: II, TEM analyses of phase evolution, *J. Am. Ceram. Soc.*, 81 (11): 2983-2997. http://dx.doi.org/10.1111/j.1151-2916.1998.tb02724.x.
2. Moya Corral, J. S.; Verduch, G.; (1978): The solid solution of silica in celsian, *Trans. J. Br. Ceram. Soc.*, 77 (2): 40-44.
3. Lee, K. -T.; Aswath, P. B.; (2003): Role of mineralizers on the hexacelsian to celsian transformation in the barium aluminosilicate (BAS) system, *Mater. Sci. Eng.*, A 352 (1-2): 1-7. http://dx.doi.org/10.1016/S0921-5093(02)00118-1.
4. Khater, G. A.; Idris, M. H.; (2007): Role of TiO_2 and ZrO_2 on crystallizing phases and microstructure in Li, Ba aluminosilicate glass, *Ceram. Int.*, 33 (2): 233-238. http://dx.doi.org/10.1016/j.ceramint.2005.08.016.
5. Lee, K. N.; (2000): Current status of environmental barrier coatings for Si-Based ceramics, *Surf. Coat. Technol.*, 133-134: 1-7. http://dx.doi.org/10.1016/S0257-8972(00)00889-6.
6. Sandhage, K. H.; Hamish, L. F.; (1995): *Synthesis of High-Temperature, Monolithic Ceramic Bodies and Ceramic-Matrix Composites by the Oxidation of Solid Metal-Bearing Precursors (SMP)*, Ohio State University, Columbus Department of Materials Science and Engineering, Columbus, Ohio, USA.
7. Debsikdar, J. C.; Sowemimo, O. S.; (1992): Effect of zirconia addition on crystallinity, hardness, and microstructure of gel-derived barium aluminosilicate $BaAl_2Si_20_8$, *J. Mater. Sci.*, 27 (19): 5320-5324. http://dx.doi.org/10.1007/BF02403837.
8. Allemeh, S. M.; Sandhage, K. H.; Fraser, H. L.; (1996): Synthesis of near net-shaped, celsian-bearing ceramics by the oxidation of solid, metal-bearing precursors (SMP). In *Processing and Fabrication of Advanced Materials IV, Minerals, Metals and Materials Society*, USA, pp. 867-879.
9. Nordlie, L. A.; (1997): Celsian-Zirconia Compositions, *US Patent No. 4,018,614*.
10. Nordmann, A.; Cheng, Y. -B.; Muddle, B. C.; (1995): Preparation of dispersed zirconia barium aluminosilicate composites, *J. Eur. Ceram. Soc.*, 15 (8): 787-794. http://dx.doi.org/10.1016/0955-2219(95)00042-S.
11. Sandhage, K. H.; Allameh, S. M.; Fraser, H. L.; (1995): A Novel Solid Metal-Bearing Precursor (SMP) Route to Near Net-Shaped Alkaline-Earth Aluminosilicates. In Galassi, C. (ed.), *Fourth Euro-Ceramics: Basic Science*

- *Developments in Processing of Advanced Ceramics - I*, Gruppo Editoriale Faenza Editrice, Faenza, Italy, pp. 499-506.
12. Yu-Feng, L.; Yong-Guo, D.; Jia-Yu, X.; Wei-Jun, Z.; Jian-Feng, W.; Guang, Y.; Yue-Ran, W.; (2008): Effect of ZrO_2 on crystallization and phase transformation in low-temperature processed BaO-Al_2O_3-SiO_2 glass-ceramics, *J. Inorg. Mater.*, 23 (1): 159-164. http://dx.doi.org/10.3724/SP.J.1077.2008.00159.
13. Bosković, S.; Kosanović, D.; Bahloul-Hourlier, Dj.; Thomas, P.; Kiss, S. J.; (1999): Formation of celsian from mechanically activated $BaCO_3$-Al_2O_3-SiO_2 mixtures, *J. Alloys Compd.*, 290 (1-2): 230-235. http://dx.doi.org/10.1016/S0925-8388(99)00091-2.
14. Long-González, D.; López-Cuevas, J.; Gutierrez-Chavarría, C. A.; Pena, P.; Baudín, C.; Turrillas, X.; (2010): Synthesis of monoclinic celsian from coal fly ash by using a one-step solid-state reaction process, *Ceram. Int.*, 36 (2): 661-672. http://dx.doi.org/10.1016/j.ceramint.2009.10.008.
15. Standard specification for coal fly ash and raw or calcined natural pozzolan for use in concrete. In *ASTM C 618-03 (2003)*, ASTM International, West Conshohocken, PA., USA.
16. Chung, F. H.; (1974): Quantitative interpretation of X-ray diffraction patterns of mixtures, I. Matrix-flushing method for quantitative multicomponent analysis, *J. Appl. Crystallogr.*, 7 (6): 519-525. http://dx.doi.org/10.1107/S0021889874010387.
17. Ramos-Ramírez, M. V.; López-Cuevas, J.; Rodríguez-Galicia, J. L.; Rendón-Angeles, J. C.; (2014): Solid state reaction synthesis of $Ba_{0.75}Sr_{0.25}AlSi_2O_8$ - Al_2O_3 ceramic composites from mechanically activated precursor mixtures, accepted for publication in the *Bol. Soc. Esp. Ceram. Vidr.*, 53 (3): 121-132. http://dx.doi.org/10.3989/cyv.162014.
18. Doghmane, M.; Hadjoub, F.; Doghmane, A.; Hadjoub, Z.; (2007): Approaches for evaluating Young's and shear moduli in terms of a single SAW velocity via the SAM technique, *Mater. Lett.*, 61 (3): 813-816. http://dx.doi.org/10.1016/j.matlet.2006.05.080.
19. Standard test method for flexural modulus of elasticity of dimension stone. In *ASTM C 1352-96 (2002)*, ASTM International, West Conshohocken, PA., USA.
20. Standard test method for flexural strength of advanced ceramics at ambient temperature. In *ASTM C 1161-02c (2002)*, ASTM International, West Conshohocken, PA., USA.
21. Standard for Fracture Toughness Testing. In *ASTM STP601-76 (1976)*, ASTM International, West Conshohocken, PA., USA.
22. Barsoum, M.W. (1997): *Fundamentals of ceramics*, McGraw Hill, N.Y., USA.
23. Standard Test Method for Microindentation Hardness of Materials. In *ASTM E384-99 (2003)*, ASTM International, West Conshohocken, PA., USA.
24. Criado, J. M.; González, F.; Morales, J.; (1979): Alteration of kinetics and thermodynamics of thermal decomposition of alkaline-earth carbonates induced by grinding, *Thermochim. Acta*, 32 (1-2): 99-110. http://dx.doi.org/10.1016/0040-6031(79)85097-2.
25. Criado, J. M.; Dianez, M. J.; Morales, J.; (2004): Influence of the mechanical treatment on the structure and the thermal stability of alkaline-earth carbonates, *J. Mater. Sci.*, 39 (16-17): 5189-5193. http://dx.doi.org/10.1023/B:JMSC.0000039208.65083.c7.
26. Berbenni, V.; Marini, A.; Bruni, G.; (2001): Effect of mechanical milling on solid state formation of $BaTiO_3$ from $BaCO_3$-TiO_2 (rutile) mixtures, *Thermochim. Acta*, 374 (2): 151-158. http://dx.doi.org/10.1016/S0040-6031(01)00505-6.
27. Berbenni, V.; Marini, A.; Bruni, G.; (2001), Effect of mechanical activation on the preparation of $SrTiO_3$ and Sr_2TiO_4 ceramics from the solid state system $SrCO_3$-TiO_2, *J. Alloys Compd.*, 329 (1): 230-238. http://dx.doi.org/10.1016/S0925-8388(01)01574-2.
28. Berbenni, V.; Marini, A.; (2002): Synthesis of $Sr_xBa_{(1-x)}TiO_3$ solid solutions from the mechanically activated system $BaCO_3$-$SrCO_3$-TiO_2, *Z. Naturforsch. B*, 57 (8): 859-864.
29. Baláž, P.; Briancin, J.; Bastl, Z.; Medvecký, L.; Šepelák, V.; (1994): Properties of mechanochemically pretreated precursors of doped $BaTiO_3$ ceramics, *J. Mater. Sci.*, 29 (18): 4847-4851. http://dx.doi.org/10.1007/BF00356532.
30. Baláz, P.; Plešingerová, B.; (2000): Thermal properties of mechanochemically pretreated precursors of $BaTiO_3$ synthesis, *J. Therm. Anal. Calorim.*, 59 (3): 1017-1021. http://dx.doi.org/10.1023/A:1010103231689.
31. Christahl, M.; Anton, S.; (1984): The thermal properties of group II metal hydroxides and of the octa-hydrates of strontium and barium hydroxide, *Int. J. Hydrogen Energy*, 9 (7): 603-607. http://dx.doi.org/10.1016/0360-3199(84)90240-4.
32. López-Badillo, C. M.; López-Cuevas, J.; Rodríguez-Galicia, J. L.; Pech-Canul, M. I.; (2013): Synthesis and characterization of $BaAl_2Si_2O_8$ using mechanically activated precursor mixtures containing coal fly ash, *J. Eur. Ceram. Soc.*, 33 (15-16): 3287-3300. http://dx.doi.org/10.1016/j.jeurceramsoc.2013.05.014.
33. Maitra, A. M.; Foger, K.; (1994): Identification of solid solutions and other phases in strontium and barium catalysts containing oxides of magnesium, aluminum or silicon as additive. II. Catalyst characterisation, *Appl. Catal. A*, 114 (1): 83-107. http://dx.doi.org/10.1016/0926-860X(94)85110-7.
34. Hemberger, Y.; Berthold, C.; Nickel, K. G.; (2012): Wetting and corrosion of yttria stabilized zirconia by molten slags, *J. Eur. Ceram. Soc.*, 32 (11): 2859-2866. http://dx.doi.org/10.1016/j.jeurceramsoc.2011.12.005.
35. López-Cuevas, J.; Long-González, D.; Gutiérrez-Chavarría, C. A.; (2012): Effect of milling time on the physical and mechanical properties of celsian-mullite composites synthesized from coal fly ash. In *MRS Proceedings Vol. 1373*, Cambridge University Press, USA, pp. 43-52.
36. Peng, F.; Liang, K.; Hu, A.; Shao, H.; (2004): Nano-crystal glass-ceramics obtained by crystallization of vitrified coal fly ash, *Fuel*, 83 (14): 1973-1977. http://dx.doi.org/10.1016/j.fuel.2004.04.008.
37. Ersoy, B.; Kavas, T.; Evcin, A.; Başpınar, S.; Sarıışık, A.; Önce, G.; (2008): The effect of $BaCO_3$ addition on the sintering behavior of lignite coal fly ash, *Fuel*, 87 (12): 2563-2571. http://dx.doi.org/10.1016/j.fuel.2008.03.012.
38. Guillem Villar, M. C.; Guillem Monzonís, C.; (1984): Kinetics and mechanism of formation of the amorphous phase from barium carbonate and kaolin, *Thermochim. Acta*, 73 (1): 67-78. http://dx.doi.org/10.1016/0040-6031(84)85177-1.
39. Sharif, A. A.; Imamura, P. H.; Mitchell, T. E.; Mecartney, M. L.; (1998): Control of grain growth using intergranular silicate phases in cubic yttria stabilized zirconia, *Acta Mater.*, 46 (11): 3863-3872. http://dx.doi.org/10.1016/S1359-6454(98)00080-9.
40. Manna, M. F.; Grandstaff, D. E.; Ulmer, G. C.; Vicenzi, E. P.; (2001): The chemical durability of yttria-stabilited ZrO_2 pH and O_2 geothermal sensors. In R. Cidu (ed.), *Proceedings of the Tenth International Symposium on Water–Rock Interaction*, Balkema, Rotterdam, The Netherlands, pp. 295-299.
41. Satapathy, L. N.; (2000): A study on the mechanical, abrasion and microstructural properties of zirconia-fly ash material, *Ceram. Int.*, 26 (1): 39-45. http://dx.doi.org/10.1016/S0272-8842(99)00017-6.
42. Kato, K.; Araki, N.; (1986): The corrosion of zircon and zirconia refractories by molten glasses, *J. Non-Cryst. Solids*, 80 (1): 681-687. http://dx.doi.org/10.1016/0022-3093(86)90462-X.
43. Krämer, S.; Yang, J.; Levi, C. G.; Johnson, C. A.; (2006): Thermochemical interaction of thermal barrier coatings with molten CaO-MgO-Al_2O_3-SiO_2 (CMAS) deposits, *J. Am. Ceram. Soc.*, 89 (10): 3167-3175. http://dx.doi.org/10.1111/j.1551-2916.2006.01209.x.
44. Mohan, P.; Yuan, B.; Patterson, T.; Desai, V.; Sohn, Y.; (2008): Degradation of yttria stabilized zirconia thermal barrier coatings by molten CMAS (CaO-MgO-Al_2O_3-SiO_2) deposits, *Mater. Sci. Forum*, 595: 207-212. http://dx.doi.org/10.4028/www.scientific.net/MSF.595-598.207.
45. Wu, J.; Guo, H. -B.; Gao, Y. -Z.; Gong, S. -K.; (2011): Microstructure and thermo-physical properties of yttria stabilized zirconia coatings with CMAS deposits, *J. Eur. Ceram. Soc.*, 31 (10): 1881-1888. http://dx.doi.org/10.1016/j.jeurceramsoc.2011.04.006.

Recibido: 04/02/2014
Recibida versión corregida: 06/04/2014
Aceptado: 11/04/2014